INSTITUTE OF PHYSICS PUBLISHING NETWORK: COMPUTATION IN NEURAL SYSTEMS

Network: Comput. Neural Syst. **12** (2001) 473–492 PII: S0954-898X(01)25411-6

Pattern recognition in a compartmental model of a CA1 pyramidal neuron

Bruce P Graham[1]

Institute for Adaptive and Neural Computation, Division of Informatics, University of Edinburgh, 5 Forrest Hill, Edinburgh EH1 2QL, UK

E-mail: B.Graham@ed.ac.uk and b.graham@cs.stir.ac.uk

Received 24 April 2000, in final form 15 February 2001
Published 15 August 2001
Online at stacks.iop.org/Network/12/473

Abstract

Computer simulation of a CA1 hippocampal pyramidal neuron is used to estimate the effects of synaptic and spatio-temporal noise on such a cell's ability to accurately calculate the weighted sum of its inputs, presented in the form of transient patterns of activity. Comparison is made between the pattern recognition capability of the cell in the presence of this noise and that of a noise-free computing unit in an artificial neural network model of a heteroassociative memory. Spatio-temporal noise due to the spatial distribution of synaptic input and quantal variance at each synapse degrade the accuracy of signal integration and consequently reduce pattern recognition performance in the cell. It is shown here that a certain degree of asynchrony in action potential arrival at different synapses, however, can improve signal integration. Signal amplification by voltage-dependent conductances in the dendrites, provided by synaptic NMDA receptors, and sodium and calcium ion channels, also improves integration and pattern recognition. While the biological sources of noise are significant when few patterns are stored in the associative memory of which the cell is a part, when large numbers of patterns are stored the noise from the other stored patterns comes to dominate the pattern recognition process. In this situation, the pattern recognition performance of the pyramidal cell is within a factor of two of that of the computing unit in the artificial neural network model.

(Some figures in this article are in colour only in the electronic version)

1. Introduction

The ability of a neuron to discriminate different patterns of synaptic input is potentially disrupted by a variety of forms of noise. Incoming signals from other neurons are subject

[1] Current address: Department of Computing Science and Mathematics, University of Stirling, Stirling FK9 4LA, UK.

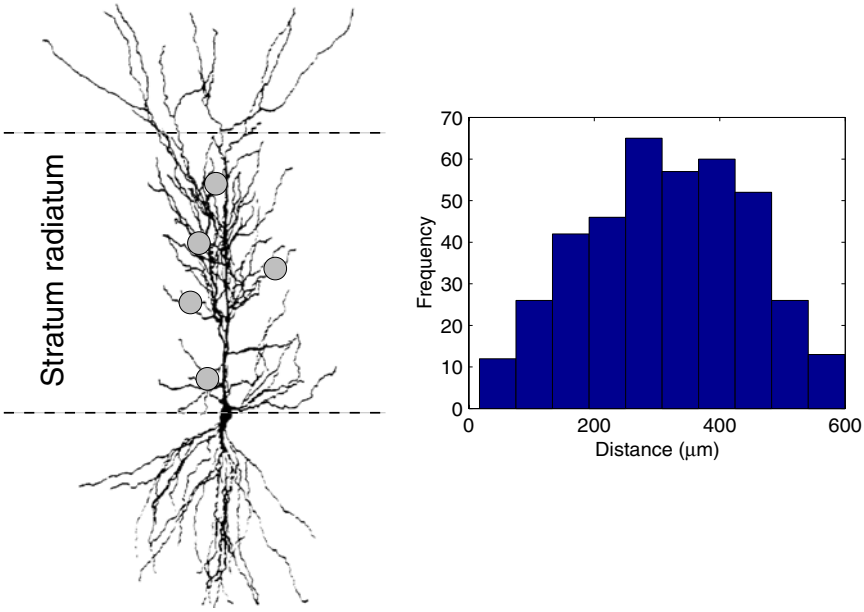

Figure 1. Schematic diagram of the CA1 pyramidal cell, showing the section of dendritic tree throughout which synaptic input was distributed (*stratum radiatum*). Circles show locations of particular synapses used to estimate effects of distance on EPSPs. The distribution of dendritic distances from the soma in *stratum radiatum* is shown on the right.

to different transmission delays, synaptic transmission is unreliable and the postsynaptic response may be affected by quantal variance (QV). Problems arise with the spatio-temporal integration of synaptic signals distributed across an extensive dendritic tree. This paper investigates the ability of a CA1 pyramidal cell to act as a pattern recognition device, given these potential sources of noise. A detailed compartmental model of a pyramidal cell is used to estimate the likely effect of the spatial distribution of synaptic input, temporal synchrony and asynchrony between inputs, and intrinsic variation in synaptic EPSP amplitudes (QV) on synaptic integration.

Cortical pyramidal neurons have extensive apical and basal dendritic trees that are the site of synaptic input from multiple excitatory and inhibitory pathways. The dendritic trees can serve to physically separate the inputs from different pathways and to provide local processing of inputs. However, inputs from a common pathway may still be distributed across a large section of dendritic tree. For example, in the mammalian hippocampus, Schaffer collateral inputs from CA3 pyramidal cells are distributed across *stratum radiatum* in the apical dendrites of a CA1 pyramidal cell (figure 1). Individual synapses may differ by several hundred micrometres in their distance from the cell body (soma). For a passive dendritic tree, the amplitude of an EPSP at the soma decreases and its time course lengthens with the distance from the soma of the originating synapse. Thus different synapses will have different abilities to influence the firing, or output, of the neuron. While this may be desirable between separate input pathways, within a common pathway it is arguable that each synapse should play an equal role in determining cell output (Cook and Johnston 1999). This is implicit in theoretical models that treat the CA3–CA1 connections as forming a heteroassociative memory (McNaughton and Morris 1987, Graham and Willshaw 1997a). In this scenario, all inputs from CA3 to a CA1 pyramidal cell are initially equal, but may be strengthened or

weakened by a Hebbian learning rule to enable patterns of activity in CA3 to be associated with patterns of activity in CA1. For Hebbian learning to have the desired effect it is essential that all the synaptic connections have the potential to equally participate in firing the CA1 neuron. It is within this context that the pattern recognition capabilities of the CA1 neuron are considered.

Experimental recordings from CA1 pyramidal cells indicate much less variation in the amplitude of the somatic response to proximal (near) and distal (far away) synaptic input than that predicted by the passive dendritic cable model (Magee and Cook 2000, Stricker *et al* 1996, Turner 1988, Andersen *et al* 1980). This implies either that synaptic conductance increases with distance so that the synaptic EPSP amplitude also increases (Magee and Cook 2000, Stricker *et al* 1996), or that voltage-gated ion channels within the dendritic tree act to boost distal synaptic input (Cook and Johnston 1997, 1999, Gillessen and Alzheimer 1997, Lipowsky *et al* 1996, Magee and Johnston 1995). Both of these possibilities are explored here.

An important question when building a functional model of a biological neural network is the exact form of the signals being passed from neuron to neuron. Previous work concerned with spatio-temporal integration and its effect on associative memory performance has considered activity to be represented by continuous firing at a particular mean frequency on each input axon (Cook and Johnston 1997, Graham and Willshaw 1997b). While this has theoretical advantages in being able to treat the postsynaptic response to inputs as steady-state conductance changes when calculating the requirements for voltage-gated ion channels to remove the effects of synaptic location (Cook and Johnston 1999), it is arguably unrealistic. Other models of associative memory in hippocampus and neocortex consider each cycle of a gamma (40 Hz) frequency oscillation to be a recall step (Jensen *et al* 1996, Lisman and Idiart 1995, Menschik and Finkel 1998). In this scenario, a postsynaptic neuron is likely to receive at most a single AP from an active presynaptic neuron within a gamma cycle. The postsynaptic neuron must perform rapid (within 25 ms) recognition of the incoming pattern of activity represented by these single action potentials arriving more or less synchronously at different synapses. It is this scenario that is employed here, with attention being paid to the effects of synchronous arrival of action potentials (APs) on subsequent signal integration. The CA1 neuron is assumed to receive at most a single synaptic contact from a particular CA3 cell (Bolshakov and Siegelbaum 1995) and an AP causes the release of at most a single vesicle of neurotransmitter (Stevens and Wang 1995).

The amplitude of the EPSP at a synapse due to the release of a vesicle of neurotransmitter may vary from AP to AP. This is known as QV. Estimates of the amount of variation range from it being negligible (CV $< 10\%$) (Stricker *et al* 1996) to quite large (CV $= 30\%$) (Bolshakov and Siegelbaum 1995, Forti *et al* 1997, Turner *et al* 1997). The effects on signal integration and subsequent memory performance of large QV are investigated.

The computer simulations presented here demonstrate that these neurobiological forms of noise may significantly affect signal integration. However, even with transient signals, active dendritic processes can act to ameliorate spatial and temporal effects that degrade signal integration. Futhermore, the results indicate that actually the noise due to the other stored patterns may dominate the pattern recognition process and so be the final determinant of associative memory performance in networks of pyramidal cells. Thus artificial neural networks, in which neurobiological noise is absent, are still reasonable models of associative memory networks in the brain. Estimates of memory capacity from such models (Bennett *et al* 1994, Treves and Rolls 1994, Graham and Willshaw 1997a) may only overestimate by a factor of around two the capacity achievable in a neurobiological system.

Some of this paper has been presented in abstract form (Graham 1999).

2. The model

2.1. Compartmental model

A detailed compartmental model of a rat CA1 pyramidal neuron (figure 1, Major *et al* 1993) was used to investigate the postsynaptic integration of transient signals in the form of individual APs arriving more or less synchronously at spatially distributed synapses. Neurobiological components activated by such transient signals, namely AMPA and NMDA receptors, and dendritic sodium and calcium channels (Gillessen and Alzheimer 1997, Lipowsky *et al* 1996, Magee *et al* 1998, Magee and Johnston 1995), were included. The model was simulated using NEURON (Hines and Carnevale 1997) and the technical details are given in the appendix.

In the model, excitatory synapses, containing both AMPA and NMDA receptors, are distributed randomly throughout the proximal apical dendritic tree, corresponding to Schaffer collaterals from CA3 neurons synapsing in *stratum radiatum*. Dendritic distances from the soma for *stratum radiatum* range up to 600 μm, with most of the tree lying between 200 and 500 μm (figure 1). A pattern of input to the cell consists of a number of individual APs arriving more or less synchronously at the spatially distributed synapses. The cell is at a steady state before the arrival of the APs, at its resting potential of -65 mV. The value used for membrane resistance includes longer-term events, such as background synaptic activity and slowly (in)activating ion channels.

Three cases for spatio-temporal integration are considered.

(1) *Uniform.* All synapses have the same AMPA-receptor-mediated peak conductance (no NMDA component) and propagation of EPSPs along the dendrites is passive.
(2) *Scaled.* Propagation of EPSPs is still passive, but synaptic conductances are scaled with distance so that any synapse produces a somatic EPSP with the same amplitude irrespective of its location.
(3) *Amplified.* Three types of voltage-activated conductance are employed as amplifiers to boost distal EPSPs; they are included individually and in combination:

(1) NMDA receptors, colocalized at the synapses with the AMPA receptors;
(2) persistent sodium channels, uniformly distributed throughout *stratum radiatum* and
(3) low-voltage-activated (LVA), inactivating calcium channels (T-type), also uniformly distributed in *stratum radiatum*.

The active conductances span a range of voltage activations and time courses. All are activated by synchronous EPSPs that are of sufficient amplitude so as to generate somatic APs, and they activate fast enough to affect the amplitude and time course of the EPSPs. The persistent sodium channels have the lowest voltage activation threshold, and the calcium channels the highest. Only the calcium channels show significant inactivation during the time course of the EPSPs. Details of these conductance models are given in the appendix. In addition, some simulations include an A-type potassium conductance and an H-type mixed cation conductance, both of which are prominent in the apical dendritic trees of these pyramidal cells (Magee 1999, Hoffman *et al* 1997).

2.2. Discrimination of the number of active inputs

The basic ability of the pyramidal cell to recognize different patterns of input rests on its ability to discriminate between different numbers of active inputs. The response of the cell to different numbers of APs is investigated. Patterns that should be recognized by the cell consist of 200 active inputs represented by single APs arriving at different synapses. This level of activity

generates a somatic depolarization of around 20 mV and would be sufficient to cause the cell to fire its own AP and thus 'recognize' the pattern. Fewer active inputs should not cause the cell to fire. This was tested by including fast sodium and potassium channels (as used by Bernander *et al* 1994a) in the soma and using a constant hyperpolarizing current injection to set a threshold, mimicking the putative role of somatic inhibition. There was a very strong correlation between the amplitude of the somatic EPSP and the firing of the cell, indicating that the EPSP amplitude is the determining factor for 'pattern recognition' (results not shown). Thus the EPSP amplitude is used as the measure of the cell's response to an input pattern and AP firing by the cell is not included in the simulations presented here.

For a particular number of active inputs, there is variation in the somatic EPSP amplitude depending on the spatial location of the synapses. Thus the cell's response to two different input patterns both of which it should recognize will vary slightly. The distribution of EPSP amplitudes produced by patterns of 200 active inputs may overlap with the distributions from lower numbers of active inputs and so reduce the cell's ability only to recognize patterns of 200 inputs. The cell's discrimination between different numbers of active inputs can be assessed by measuring the signal-to-noise ratio (S/N) between respective distributions of somatic EPSP amplitudes (Dayan and Willshaw 1991):

$$\mathrm{S/N} = \frac{1}{2}\frac{(\mu_\mathrm{h} - \mu_\mathrm{l})^2}{(\sigma_\mathrm{h}^2 + \sigma_\mathrm{l}^2)}$$

where μ_h (μ_l) and σ_h^2 (σ_l^2) are the mean and variance of the EPSP amplitude from the higher (lower) number of active inputs, respectively. In the following results, the distribution of peak voltages due to 100 and 200 active inputs from 100 simulations with different spatial distributions of synapses are compared using this S/N. The higher the ratio, the better able the cell is to discriminate between 100 and 200 inputs.

2.3. Pattern recognition in an associative memory

In a more realistic situation, the pattern recognition ability of the cell is compared with that of a computing unit from an artificial neural network model of associative memory (Cook and Johnston 1997). Hebbian learning is employed to associate both the cell and the computing unit with the same set of input patterns. The simple neural network model of associative memory that is used here is the associative net (Willshaw *et al* 1969). In this model, synaptic weights are binary. During pattern storage, the connection between two units is given a weight of one if both units are active for a particular input–output pattern pair (*clipped* Hebbian learning). During recall, an output unit must recognize an input pattern on the basis of the number of active inputs it is connected to by a weight of one. Thus the output unit must be able to accurately count the number of active inputs impinging upon it.

An associative net consisting of 8000 input units connected to eight output units was used. The number of inputs impinging on each output unit is of the same order as the number of Schaffer collateral synapses on a CA1 pyramidal cell. Sixty random binary pattern pairs, each consisting of 200 active input and four active output units, were stored in the memory. Each output unit was associated on average with 30 of the input patterns. Memory performance is assessed by applying each input pattern to every output unit and collecting the summed inputs calculated by each output unit. This produces distributions of sums due to patterns that should be recognized (*high* patterns) and due to those that should not (*low* patterns). The separation of the distributions is measured using the S/N described above.

2.4. Pattern recognition in the pyramidal cell

To compare the memory performance of the pyramidal cell with that of the computing units in the associative net it was necessary to represent both stored patterns and synaptic weights in a form suitable for the pyramidal cell. The 8000 inputs were represented by spatially distributed synapses. Binary synaptic weights corresponded to the presence or absence of synaptic conductances, depending on whether a synapse was potentiated by Hebbian learning, or not, respectively. A binary input pattern was represented by a single AP on each active (non-zero) input line, with the APs being more or less synchronous between input lines.

To compare the pattern recognition performance of the cell with an output unit in the associative net, the weight matrix resulting from the storage of 60 pattern pairs for that output unit was used to set the synaptic weights in the pyramidal cell model. Then all of the input patterns stored in the associative net were presented to the cell in the form of APs, as described above. The distributions of somatic EPSP amplitudes due to *high* and *low* patterns were collected and compared using the S/N to give a performance measure that is directly comparable with the performance of the output unit in the associative net. The pyramidal cell is compared with all eight of the output units in turn.

3. Results

3.1. Signal loss in the dendritic tree

One focus of this paper is the distortion of input signals as they travel from a synapse along the dendritic tree to the final site of integration in the soma. Attenuation of signals in the passive dendritic tree of a CA1 pyramidal cell has been studied in detail elsewhere (Mainen *et al* 1996). Figure 2 shows examples of EPSPs generated at different distances in the apical dendritic tree and the subsequent voltage response at the soma, when average values are used for the passive membrane characteristics (see the appendix). Distal signals ($\approx$500 μm) are attenuated more than 120-fold during propagation to the soma and the peak of the EPSP is delayed by about 8 ms from its peak at the synapse. Recent experimental results (Magee and Cook 2000) indicate that attenuation may be significantly less than this in such cells. The level of attenuation used here results from the use of a relatively high value for axial resistance ($R_a = 200\ \Omega$ cm) and provides a severe test for the amplification properties of active channels, to be considered below.

While synaptic EPSPs are finished after 20 ms, the somatic response lasts around 100 ms. With *uniform* synaptic conductances (figures 2(*a*) and (*b*)), somatic EPSPs have similar amplitude from about 30 ms onwards, irrespective of the synaptic location. In contrast, with *scaled* conductances, the amplitudes of somatic EPSPs from distal synapses are elevated for the full extent of the EPSP. This has implications for the integration of signals from synapses distributed across the dendritic tree.

With *uniform* synaptic conductances the somatic amplitude decreases exponentially with synaptic distance. There is a trend towards increasing synaptic amplitude with distance due to reduction in dendritic diameters and a decrease in electrical load from the large soma and proximal apical trunk. This is accentuated in the *scaled* case due to increasing synaptic conductance with distance. A simple linear increase in AMPA conductance with distance, from around 0.5 nS peak conductance at 100 μm up to 1.8 nS at 500 μm, provides a similar EPSP amplitude in the soma, irrespective of synaptic distance. This range of conductances is well within the bounds of estimates for Schaffer collateral synapses (Stricker *et al* 1996). Note that the voltage-gated channels used to boost population inputs (*amplified* case) have little effect on individual EPSPs.

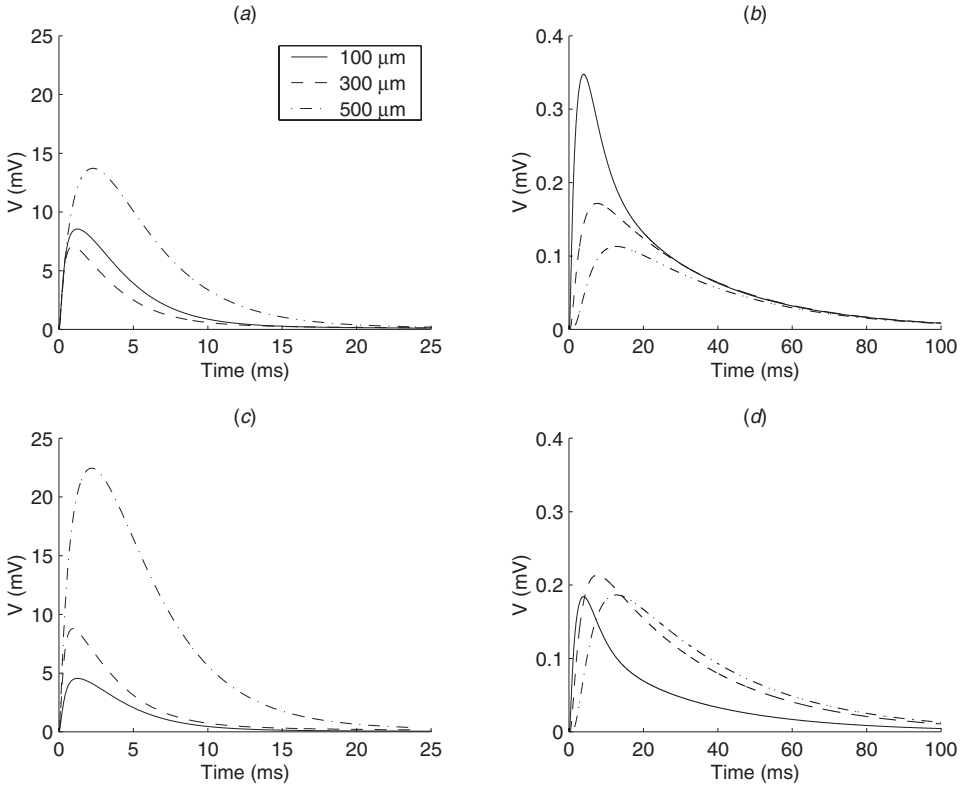

Figure 2. EPSPs at the synapse (*a*), (*c*) and subsequently at the soma (*b*), (*d*) for synapses at different distances from the cell body. (*a*), (*b*) Passive dendritic tree with uniform synaptic conductances. (*c*), (*d*) Conductances scaled to give similar EPSP amplitudes in the soma.

3.2. Discrimination of inputs

3.2.1. Synchronous arrival of action potentials. We are interested in the cell's ability to discriminate different levels of population input activity. Consider initially the somatic voltage response to different numbers of APs arriving synchronously at spatially distributed synapses. Examples of somatic voltage responses to either 100 or 200 APs for the *uniform* case are shown in figure 3(*a*). While the voltage waveforms due to a particular number of APs are very similar in shape, there is variation in the amplitude, depending on the spatial distribution of the synapses. This is the result of differing levels of EPSP attenuation and soma arrival times for synapses that are different distances from the cell body. The distributions of somatic population EPSP amplitudes are shown in figure 3(*b*). While in this case it is clear that the cell can distinguish between 100 and 200 APs, there will be overlap in the responses to closer numbers of APs.

A measure of how well the cell can discriminate the responses is given by the S/N of the distributions. The S/N of a number of different situations, with synchronous AP arrival, is shown by the left-hand column of each histogram in figure 4. Scaling of synaptic conductance with distance, or amplification of EPSPs by a voltage-activated conductance, acts to increase the S/N significantly compared to the *uniform* case. When adding the different voltage-gated conductances individually to the dendritic tree, the NMDA-receptor-mediated synaptic

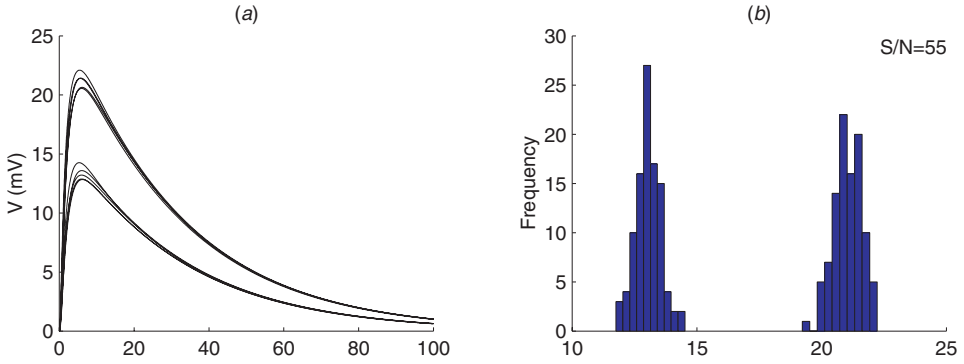

Figure 3. Population EPSPs at the soma due to 100 or 200 active synapses for the *uniform* case. (*a*) Example EPSPs. (*b*) Distribution of EPSP amplitudes and the resultant S/N.

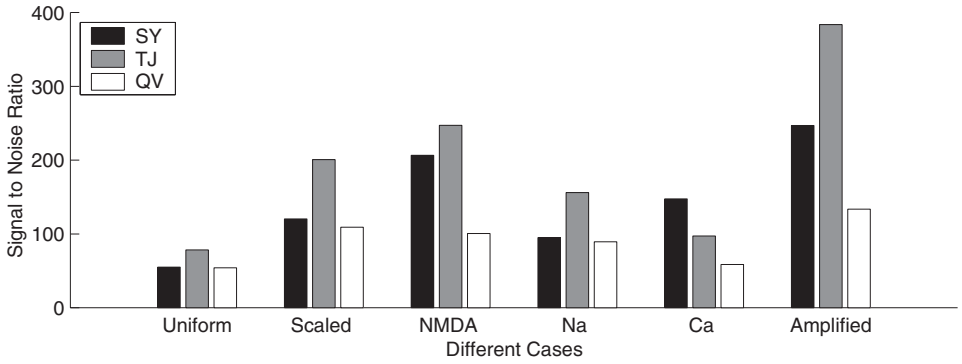

Figure 4. S/N between EPSP amplitudes due to 100 or 200 active synapses for the different cases. Amplifying conductances are included individually (NMDA, Na and Ca; with AMPA synapses without *scaling*) and in combination (amplified; includes *scaling*). The three columns for each case are: SY, synchronous APs: TJ, temporal jitter (time window of 20 ms); and QV, temporal jitter plus QV (CV = 0.3).

conductance works best, providing a fourfold increase in S/N. A fivefold increase was obtained when *scaling* was combined with all of the voltage-dependent conductances (*amplified* case).

The effects of the different amplifying conductances are illustrated by considering the mean and standard deviation of the somatic EPSP amplitudes due to different numbers of synchronous APs, as shown for the different cases in figure 5. *Scaling* and the NMDA conductance both decrease the standard deviation of the EPSP amplitude for a particular number of active synapses (figure 5(*b*)) due to a reduction in the spatial variation of individual EPSP amplitudes. Thus the increase in S/N between 100 and 200 APs in these cases is due in part to a narrowing of the spread of the population EPSP amplitude distributions. The NMDA component of the synaptic conductance also acts to linearize the mean EPSP amplitude for different numbers of active synapses (figure 5(*a*)). The combined EPSPs from higher numbers of activated synapses are boosted more than smaller EPSPs due to the voltage-activated nature of the NMDA conductance. This also increases the S/N by separating the mean amplitudes between the population EPSPs for 100 and 200 synapses.

Such effects are also seen when sodium or calcium channels are used to amplify EPSPs, and when all of the active conductances are combined (figures 5(*c*), (*d*)). The persistent

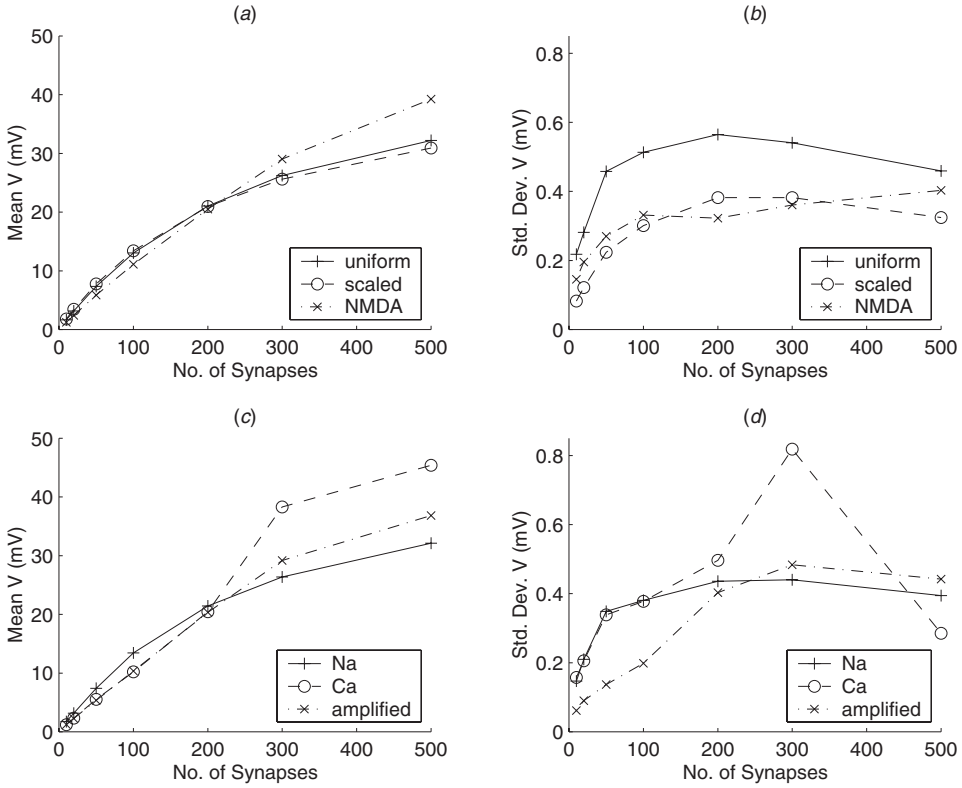

Figure 5. Mean (*a*), (*c*) and standard deviation (*b*), (*d*) of EPSP amplitudes due to different numbers of active synapses with synchronous APs. (*a*), (*b*) *Uniform*, *scaled* and *NMDA* cases; (*c*), (*d*) Na, Ca and *amplified* cases.

sodium channels are activated by both 100 and 200 active synapses and serve mostly to reduce population EPSP variance by amplifying distal individual EPSPs. The calcium channels are activated at higher voltages and boost the EPSPs of 200 synapses more than those from 100 synapses, resulting in a linearization of the mean population EPSP amplitude curve for different numbers of active synapses, as with the NMDA conductance. However, there is a significant increase in variance in EPSP amplitude for 300 active synapses, as the regenerative amplification by the calcium conductance becomes excessive and amplifies small differences in EPSP amplitude. This effect reduces for 500 synapses due to damping by a reduction in driving force of the synaptic conductances.

3.2.2. Asynchronous AP arrival. In reality, there will be variability in the transmission delays from different CA3 input cells and the firing times of these cells may not be perfectly synchronized. To test the effect of such *temporal jitter*, the arrival times of the APs at different synapses were distributed uniformly in a 20 ms time window. Surprisingly, in all cases, except for the calcium conductance alone, this significantly increased the S/N (figure 4; middle columns of each histogram). This is largely the result of a decrease in the variance of the EPSP amplitudes, as illustrated in figure 6. This is likely due to a reduction in interference between nearby synapses and a randomizing of the arrival times of near and far synaptic EPSPs at the soma.

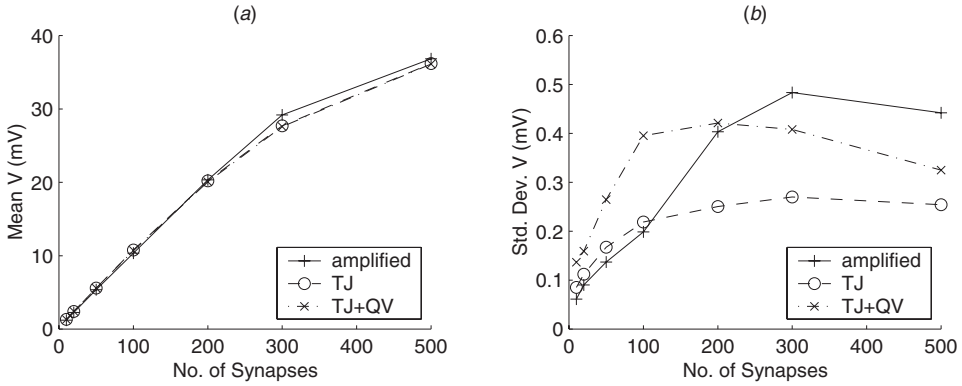

Figure 6. (*a*) Mean and (*b*) standard deviation of EPSP amplitudes due to different numbers of active synapses in the *amplified* case with either synchronous APs, asynchronous APs (TJ; time window of 20 ms), or asynchronous APs with QV (TJ + QV; CV = 0.3).

The width of the *temporal jitter* time window affects the S/N, with 20 ms being optimal for the *uniform* case. The optimum time window must depend on the time course of the underlying synaptic EPSPs. Once the window becomes too long, early synaptic EPSPs are nearly finished by the time late EPSPs arrive and their summation will be poor. The decreased performance of the calcium conductance with temporal jitter (see figure 4) is due to the fast inactivation of the conductance, resulting in early EPSPs partially inactivating the calcium amplification for later EPSPs. A certain persistence in the amplifying mechanism is thus useful in this situation, as afforded by the NMDA and persistent sodium conductances.

3.2.3. Quantal variance. Apart from spatio-temporal integration, another potentially significant source of noise in the summation process is trial-to-trial variation in EPSP amplitude at each synapse, known as QV. Introducing a random variation in the peak conductance at each synapse at the maximum level measured experimentally (coefficient of variation = 0.3) (Bolshakov and Siegelbaum 1995, Forti *et al* 1997, Turner *et al* 1997) results in a 30–60% reduction in the S/N, annulling any increase afforded by temporal jitter (figure 4, right-hand columns of each histogram). QV increases the variance in EPSP amplitudes (figure 6(*b*)). The effect of QV is most pronounced when the NMDA conductance is involved, as any variation in synaptic conductance is accentuated by the voltage-dependent nature of the NMDA component.

To compare the magnitude of noise due to QV with that from the spatial distribution of synapses, the S/N was calculated from responses with all synapses located at the soma and affected by QV (results not shown). This indicated that noise due to QV is somewhat less than that due to spatio-temporal integration of inputs in the *uniform*, synchronous AP arrival case (S/N = 220 for QV compared to 55 for the *uniform* case). QV must be twice the magnitude used here to approach the level of noise from spatially distributed synapses (Graham 1999).

3.3. Pattern recognition

The pattern recognition capability of the pyramidal cell was tested by examining its ability to distinguish between *high* and *low* patterns stored in the associative net. Firstly, the 60 stored input patterns were presented in turn to the artificial neural network model and the resulting input sum of each output unit was recorded. The distribution of sums over the 60 patterns for the first unit is shown in figure 7(*a*). Note that *high* patterns always produce a sum of 200,

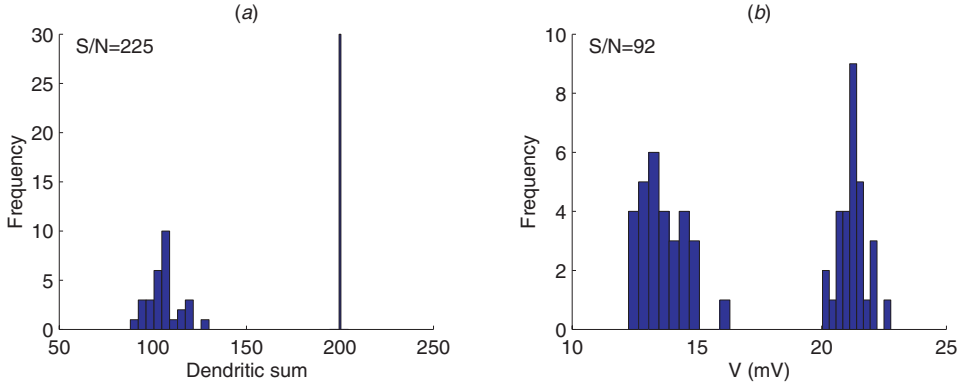

Figure 7. Distributions of input sums due to *low* and *high* patterns stored in the associative net for (*a*) a computing unit in the net (actual sums) and (*b*) the pyramidal cell (*uniform* case; sums measured as somatic EPSP amplitudes). The S/N between the distributions are shown in each figure.

while the *low* sums exhibit variability around a mean of about 100. The S/N between the *high* and *low* pattern sums is given in the figure.

For each output unit in turn, the pattern of connection weights in the net was used to set 8000 synaptic connections onto the model pyramidal cell. The 60 input patterns were then presented to the cell. The somatic EPSP amplitude was recorded for each pattern. The amplitude distributions due to *high* and *low* patterns from the *uniform* case for the cell corresponding to the first unit are shown in figure 7(*b*). Now there is variability in both the *high* and *low* sums and the S/N is about 35% of that of the computing unit.

The mean S/N of the cell compared to the S/N of an output unit was calculated across the eight output units for the different cell cases, with and without temporal jitter and QV. The results are summarized in figure 8. The S/N is 70% of that of a computing unit when EPSPs are *scaled* and *amplified*. Temporal jitter and QV now have smaller effects on performance and the performance differences between the cases are much less than when comparing 100 with 200 active synapses. In this situation, *low* patterns activate different numbers of synapses. This variability dominates the spread of *low* sums, so that the noise in the cell does not greatly increase the variance of the *low* sums compared to those for a network unit.

4. Discussion

A compartmental model of a hippocampal CA1 pyramidal neuron has been used to assess this cell's ability to accurately calculate the weighted sum of its inputs. Such an ability is necessary if the network formed by Schaffer collateral inputs from CA3 pyramidal cells onto CA1 pyramidal cells forms a heteroassociative network, as has been postulated (McNaughton and Morris 1987). This paper extends previous studies that considered the spatio-temporal integration of essentially steady-state input in the form of trains of APs (Cook and Johnston 1997, 1999, Graham and Willshaw 1997b). Here, transient inputs in the form of individual APs have been used and the effects of a variety of forms of noise have been considered. This provides an indication of the likely ability of the pyramidal cell to rapidly recognize different patterns of input, as required if the cell is a part of an associative memory network operating at gamma (40 Hz) frequency (Jensen *et al* 1996, Lisman and Idiart 1995, Menschik and Finkel 1998).

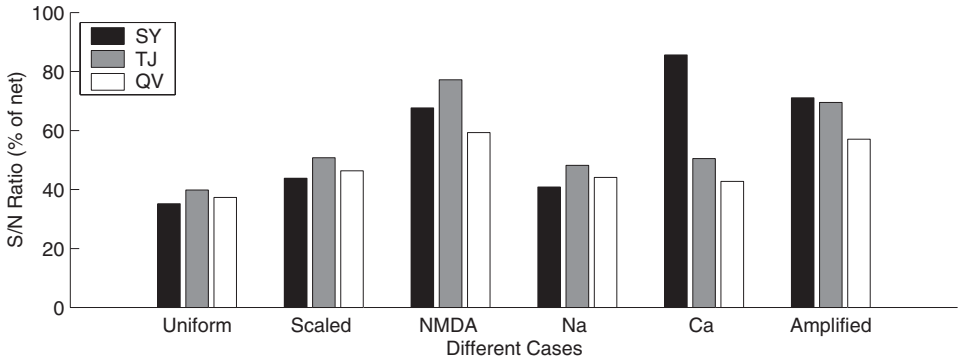

Figure 8. Average S/N between *high* and *low* pattern input sums for the different pyramidal cell cases, relative to the equivalent S/N of a computing unit. The three columns for each case are: SY, synchronous APs: TJ, temporal jitter (time window of 20 ms); and QV, temporal jitter plus QV (CV = 0.3).

Various forms of noise interfere with signal integration in neurons. Input synapses are distributed across a dendritic tree, resulting in spatio-temporal distortion of the synaptic signals as they travel to the final point of integration in the cell body. APs from different input cells will not be perfectly synchronized at the synapses, and the subsynaptic EPSP amplitude may vary from AP to AP. The effects of these different sources of noise have been investigated.

4.1. Signal attenuation and passive membrane properties

The amplitude of the voltage response at the soma when a number of synapses are activated simultaneously depends on the spatial distribution of the synapses. Variations in amplitude occur for different spatial arrangements of the same number of active synapses (figure 3). This limits the postsynaptic cell's ability to discriminate between different numbers of active synapses. The magnitude of the variation depends on the passive properties of the cell membrane. The results presented here are based on average values for resistance and capacitance ($R_m = 30$ kΩ cm^2, $R_a = 200$ Ω cm, $C_m = 1$ μF cm^{-2}) for the range estimated from experiments (Mainen *et al* 1996). Increasing the membrane resistance, R_m, does increase the S/N by reducing the attenuation of distal EPSPs. For example, using $R_m = 100$ kΩ cm^2 roughly doubles the S/N between 100 and 200 active inputs. However, it also increases the duration of the somatic response. The scenario employed here is based on the assumption that the neuron can respond to a new pattern of input on every cycle of a gamma frequency (40 Hz) oscillation, without interference from previous inputs. Thus the cell must have a low membrane resistance, providing a fast time constant. Even if the membrane itself has high resistance ($R_m = 100$ kΩ cm^2 or more), low-frequency background synaptic input (Bernander *et al* 1991) or suitably timed inhibitory input will serve to lower the effective membrane resistance. Ion channels in the dendrites, such as the A-type potassium current and the H-current, may also aid the required rapid membrane repolarization (Hoffman *et al* 1997, Magee 1999). Addition of these channels to the model (results not shown) resulted in an earlier peak in the EPSP, due to the A-current, and a shorter time course, due to inactivation of the H-current, as seen experimentally by Magee (1999). The A-type current also slightly reduced the S/N as its voltage-dependent activation served to attenuate the higher-amplitude EPSPs due to 200 active inputs more strongly than lower-amplitude EPSPs from 100 inputs, bringing the respective EPSP amplitude distributions closer together.

Perhaps more uncertain is the appropriate value of the axial resistance, R_a. Estimates range from around 50–400 Ω cm (Mainen *et al* 1996). Lowering R_a also improves the S/N by reducing the attenuation of distal inputs relative to proximal inputs. Subsynaptic voltages are also reduced and are more spatially uniform. Thus a low value of R_a increases the equivalence of spatially distributed synapses. Recent electrophysiological recordings show much less attenuation of EPSPs with distance in CA1 pyramidal cells than for the simulations here, indicating an R_a of around 70 Ω cm (Magee and Cook 2000). Higher values of R_a may be appropriate in separating out the effects of different input pathways located in different sections of a dendritic tree. Scaling of synaptic conductances or amplification of EPSPs could then equilibrate the synapses of a common input pathway.

4.2. Scaling and amplification

In contrast to previous studies that concentrated on the possibility of signal amplification by ion channels in the dendritic tree (Cook and Johnston 1997, 1999), here a reduction in the attenuation of distal EPSPs was achieved by a simple scaling (increase) in peak synaptic conductance with distance from the soma (Magee and Cook 2000, Stricker *et al* 1996), as well as by amplification with voltage-activated ion channels (Gillessen and Alzheimer 1997, Lipowsky *et al* 1996, Magee and Johnston 1995). Both methods improved the S/N by reducing the variance in the somatic EPSP amplitudes from different spatial arrangements of the same number of active synapses. The significant difference between the methods was that scaling affected even individual EPSPs from a single activated synapse, while amplification only boosted population EPSPs where the summed amplitude reached several millivolts. In reality, a combination of scaling and amplification may be employed. The somatic response to individual synapses does not correlate with distance, implicating conductance scaling (Magee and Cook 2000, Stricker *et al* 1996). Active sodium and calcium channels in dendrites have been shown to amplify large-amplitude EPSPs in many neuronal types (De Schutter and Bower 1994, Gillessen and Alzheimer 1997, Lipowsky *et al* 1996, Magee and Johnston 1995). Here, pattern recognition was improved by the use of a combination of scaling and amplification (figures 4 and 8).

NMDA channels at synapses and a uniform density of persistent sodium channels or calcium channels throughout *stratum radiatum* was used to provide amplification. The improvement in S/N that resulted is in accord with previous modelling work that tested the use of calcium and sodium channels in this capacity (Cook and Johnston 1997). If active inputs are represented by steady-state conductance changes it is possible to calculate the channel characteristics required to eliminate location-dependent variability from the somatic response (Cook and Johnston 1999). It is unlikely that active channels could fully eliminate this variability for transient synaptic inputs. Increasing the density of the active channels does increase the S/N but, as with high R_m, the EPSP time course is significantly lengthened due to the long time course of particularly the NMDA and persistent sodium conductances. As discussed previously, inhibitory conductances and suitably timed inhibitory postsynaptic potentials (IPSPs) can act to forshorten the EPSPs.

The amplification by active channels resulted in a reduction in the variance of population EPSP amplitudes and a linearization in the summation of EPSPs. The role of active conductances in the dendrites in such linearization has been explored in other computer models (Bernander *et al* 1994a) and experimentally (Cash and Yuste 1998, 1999). Sodium, calcium and NMDA conductances may participate in this (Cash and Yuste 1999). Such amplification can also lead to local nonlinear summation and an enhancement of synaptic location-dependent variability. This can result in a neuron responding preferentially to synchronous inputs at

spatially clustered synapses (Mel 1993). With the diffuse input from large numbers of synapses used here, the entire dendritic tree is depolarized relatively uniformly and the voltage-dependent amplification serves to boost the input from higher numbers of synapses more than for smaller inputs, separating the population EPSP amplitudes for different numbers of synapses and hence increasing the S/N. This is particularly prominent for the NMDA and calcium conductances, which have a higher voltage activation threshold than the persistent sodium conductance used here.

In principle, this boosting mechanism could be applied directly to the summed EPSPs in the soma, rather than throughout the dendritic tree. Recent experiments have implicated a somatic persistent sodium current in the amplification of EPSPs near threshold (Andreasen and Lambert 1999). This was tested by adding persistent sodium channels to the soma only. This did indeed result in a considerable increase in S/N, even when the dendrites were passive (results not shown). However, there is a tradeoff with this use of regenerative channel activation for amplification. Too much amplification also leads to an increase in variance in EPSP amplitudes as small differences in amplitude are magnified (note, for example, the high variance for 300 synapses with calcium channels, shown in figure 5(*d*)). This can counteract the positive effect of increasing the separation in EPSP amplitudes for different numbers of synapses, leading to a decrease in S/N.

In summary, amplification of EPSPs by active conductances distributed diffusely within the dendritic region of synaptic input robustly improves the integration of transient inputs, provided the amplification is not too large. Exact details of the time course and voltage activation range of the active conductances are not crucial, providing activation is sufficiently fast when inputs are transient, and activation does occur in the dendritic voltage range produced by the synaptic input. Activation should last for at least the duration of transient input and the transmission times of distal EPSPs to the soma.

4.3. Temporal jitter

The asynchronous arrival of APs can also act to improve the accuracy of signal integration, provided the APs are dispersed over a suitably short period of time. Interference between nearby synaptic responses is reduced and EPSP transmission delays to the soma are randomized. The optimum time window is dependent on the time course of the EPSPs and was about 20 ms with passive dendrites. This is sufficiently short that the CA1 cell can still integrate and react to a pattern of input within one cycle of a 40 Hz oscillation. It is also compatible with the hypothesis that bursts of presynaptic APs are the fundamental input signal (Lisman 1997). Bursts in CA3 cells last less than 25 ms and, given the probabilistic nature of synaptic transmission, each burst may only produce a single postsynaptic EPSP at some time within the burst period. Thus bursting, together with low probabilities of transmitter release, can provide a suitable dispersion in time of the synaptic EPSPs.

Asynchronous APs may also maximize cell firing in response to trains of synaptic input. This is due to not wasting input during cell refractory periods, rather than by reducing synaptic saturation (Bernander *et al* 1994b). Hence very precise synchronicity of inputs is not desirable, even if the receiving neuron is acting as a 'coincidence detector'.

4.4. Quantal variance

QV at the maximum level estimated experimentally (Bolshakov and Siegelbaum 1995, Forti *et al* 1997, Turner *et al* 1997) is a major source of noise, but not as significant as that due to spatio-temporal integration. However, a neuron is unable to compensate for such noise by the use of active conductances in the same way that spatio-temporal noise can be dealt with.

If pattern recognition is a multi-step process, such as during recall in an autoassociative memory, then a small amount of synaptic noise can actually be beneficial (Amit 1989, Bennett *et al* 1994). In this situation it introduces variability into each neuron's output, that stops the network of neurons becoming stuck in false patterns of activity that do not correspond to the required stored memory.

4.5. Pattern recognition in an associative memory

In a simple pattern recognition task based on a heteroassociative memory model, a pyramidal cell including all these forms of noise may have a S/N that is 70–80% of that achieved by a noise-free network computing unit. This is achieved using only transient pattern presentation in the form of single, quasisynchronous APs on each active input. Recognition is very rapid (within 5–20 ms). Earlier work with a model neocortical pyramidal cell showed a one- to two-order-of-magnitude reduction in the S/N, when the input signals were in the form of trains of APs of a fixed mean frequency (Graham and Willshaw 1997b). With such steady-state input, active conductances can be tuned to remove location-dependent variability (Cook and Johnston 1997, 1999) and linearize the response to different numbers of inputs (Bernander *et al* 1994a). This can dramatically improve the neuron's pattern recognition performance (Cook and Johnston 1997). With the transient input signals used here, however, the neuron achieved 40% of the performance of the computing unit even without synaptic conductance scaling or amplification to combat spatial effects. This rose to between 70 and 80% with the inclusion of active conductances. The membrane properties of a neuron dictate the nature of input to which it is most responsive. It would seem that CA1 pyramidal cells are well tuned to respond to transient inputs over a time window of around 25 ms and so can plausibly recognize patterns at gamma frequency. When the basic passive characteristics are poorly matched to the input, voltage-gated ion channels distributed throughout the dendritic tree can shape the membrane properties to suit the input.

4.6. Other forms of noise

Other forms of noise will also affect a biological neuron's ability to function as a pattern recognition device. A comparison between the effects of the forms of noise considered here and other sources of noise, namely partial connectivity and probabilistic synaptic transmission, can be made by considering the variance in input sums with a mean value of 200, when the different forms of noise are present individually.

In a network such as that formed by the CA3 Schaffer collateral input onto CA1 pyramidal cells, each CA1 cell will receive input from only a small fraction of the CA3 cells. Consequently, each CA1 cell receives only a sample of the total activity in CA3. For the heteroassociative memory model this means that even input patterns that the output cell should recognize will consist of variable numbers of active inputs, rather than the fixed number used here. Suppose the CA1 cell receives connections from 5% of the CA3 cells (Bennett *et al* 1994, Bolshakov and Siegelbaum 1995). If each input pattern is represented by 4000 active CA3 cells, the mean *high* pattern input sum at the CA1 cell will be 200 active synapses with a standard deviation of 14, giving a coefficient of variation of 0.07. In the results presented here, the noisy input sums for exactly 200 active inputs have a coefficient of variation of between 0.03 and 0.06. Thus partial connectivity may represent an even more serious source of noise than spatio-temporal integration or QV. Appropriate threshold setting during recall can ameliorate the effects of partial connectivity in neural network models of associative memory (Buckingham 1991, Marr 1971). It is possible that such thresholding strategies could be employed in neurobiological networks as well (Graham and Willshaw 1995).

If the input from CA3 cells consists of single APs, rather than the bursts discussed earlier, then probabilistic transmission will also be a considerable source of noise (Allen and Stevens 1994). Suppose the CA1 cell is connected to all of the CA3 cells that belong to input patterns with which it is associated. Given that the probability that a presynaptic AP causes an EPSP is only 0.2 and the input pattern consists of 1000 active cells, the mean *high* pattern sum is again 200, but with a standard deviation of 13. If the probability of transmission is 0.8 and patterns contain 250 cells, the standard deviation reduces to 6. Thus the noise from probabilistic transmission will be similar in magnitude to the forms of noise considered here.

4.7. Summary

The work presented here demonstrates that, despite many sources of noise, a pyramidal neuron can rapidly (within 5–20 ms) recognize transiently presented patterns of input. This supports the hypothesis that networks of pyramidal cells can operate as associative memory devices and recall stored patterns at gamma (40 Hz) frequency.

Spatio-temporal dispersion of input signals, QV and variation in signal arrival times all act to distort the summation of inputs by the neuron. Increases in peak synaptic conductances with distance and boosting of distal inputs by voltage-dependent conductances act to reduce spatial variations. Preferential amplification of large signals by voltage-dependent conductances also aids discrimination of such signals from weaker inputs.

The cell's ability to act as a pattern recognition device is sufficient that a network of cortical pyramidal cells can function as an associative memory when Hebbian learning is used to store patterns by altering connection weights. As such a memory nears capacity, the noise due to other stored patterns comes to dominate the pattern recall process and the pattern recognition performance of a pyramidal cell approaches within a factor of two of that of a computing unit in an equivalent artificial neural network model. Consequently, estimates of the memory capacity of biological networks can reasonably be based on the capacity of artificial models using simple computing units.

Acknowledgments

To the MRC for financial support under PG 9119632 to Professor David Willshaw. Many thanks to Guy Major for supplying the morphology of the CA1 pyramidal cell.

Appendix. Pyramidal cell model details

Cell: rat CA1 pyramidal cell as per figure 2 of Major *et al* (1993).
Compartments: 890
Passive properties: $R_m = 30\,k\Omega\,cm^2$, $C_m = 1\,\mu F\,cm^{-2}$, $R_a = 200\,\Omega\,cm$ throughout neuron (Mainen *et al* 1996). Membrane area is adjusted to compensate for spine area.
Synapse: excitatory, AMPA and NMDA type with synaptic current

$$I_s = g_s(V - E_s)$$

where V is the local membrane potential, $E_s = 0$ mV is the synaptic reversal potential and g_s is the synaptic conductance given by

$$g_s = (1 - \alpha)g_{AMPA} + \alpha g_{NMDA}$$

where $0 \leqslant \alpha \leqslant 1$ determines the relative contributions of AMPA and NMDA receptors to the total conductance; α is 0 for AMPA-only synapses, 0.1 for AMPA and NMDA synapses with passive dendrites and 0.05 with synaptic conductance scaling or active dendrites.

The AMPA conductance is

$$g_{\mathrm{AMPA}} = \bar{g}_{\mathrm{s}} \frac{\tau_1 \tau_2}{\tau_2 - \tau_1} (\mathrm{e}^{-t/\tau_2} - \mathrm{e}^{-t/\tau_1})$$

where $\tau_1 = 0.2$ ms, $\tau_2 = 2$ ms and $\bar{g}_{\mathrm{s}} = 6$ nS gives a peak AMPA-only conductance of about 1 nS (Forti *et al* 1997, Mainen *et al* 1996).

The NMDA conductance is voltage dependent and is described by the model of Mel (1993):

$$g_{\mathrm{NMDA}} = \bar{g}_{\mathrm{s}} \frac{\mathrm{e}^{-t/\tau_2} - \mathrm{e}^{-t/\tau_1}}{1 + \mu[\mathrm{Mg}^{2+}]\mathrm{e}^{-\gamma V}}$$

where $\tau_1 = 0.66$ ms, $\tau_2 = 80$ ms, $\mu = 0.33\ \mathrm{mM}^{-1}$, $[\mathrm{Mg}^{2+}] = 1$ mM and $\gamma = 0.06\ \mathrm{mV}^{-1}$. In all simulations $\bar{g}_{\mathrm{s}}$ was set to give a peak somatic depolarization of ≈20 mV with 200 active synapses. Synapses were located directly on the dendritic membrane. Initial studies locating synapses on spines showed that the spines had only a very small quantitative effect on the voltage response (Cook and Johnston 1997).

Scaling: synaptic peak conductance, $\bar{g}_{\mathrm{s}}$ is scaled to give constant EPSP amplitude in the soma when dendrites are passive, via the empirical equation

$$\bar{g}_{\mathrm{s}} = g_0(1 + 0.020\,88d)$$

where d is the soma–synapse distance (μm) and g_0 is the maximum conductance at the soma ($\bar{g}_{\mathrm{s}} = 1$ nS gives peak somatic depolarization of ≈20 mV with 200 AMPA-only synapses).

Voltage-gated ion channels: EPSPs amplified by persistent sodium channels or calcium channels uniformly distributed throughout *stratum radiatum*, and in some simulations the EPSP time course is affected by A-type potassium channels and an H-type mixed cation current.

Persistent sodium current given by Lipowsky *et al* (1996)

$$I_p = g_p m(V - E_{\mathrm{Na}})$$

where $E_{\mathrm{Na}} = 65$ mV and activation, m is controlled by standard first-order dynamics with

$$\alpha_{\mathrm{m}} = \frac{-1.74(V - 11)}{(\exp(-(V - 11)/12.94) - 1)}$$
$$\beta_{\mathrm{m}} = \frac{0.06(V - 5.9)}{(\exp((V - 5.9)/4.47) - 1)}$$
$$\tau_{\mathrm{m}} = 1/(\alpha_{\mathrm{m}} + \beta_{\mathrm{m}})$$
$$m_\infty = 1/(1 + \exp(-(V + 49)/5)).$$

A peak conductance of $\bar{g}_p = 0.01\ \mathrm{mS\ cm}^{-2}$ was used when this was the only active conductance, being reduced to $0.005\ \mathrm{mS\ cm}^{-2}$ when other voltage-gated conductances were present. In some simulations the current was only added to the soma, in which case $\bar{g}_p = 0.2\ \mathrm{mS\ cm}^{-2}$ was used.

Low-voltage-activated, inactivating calcium current given by Lipowsky *et al* (1996), Warman *et al* (1994)

$$I_{\mathrm{Ca}} = g_{\mathrm{Ca}} m^2 h(V - E_{\mathrm{Ca}})$$

where $E_{Ca} = 80$ mV and (in)activation kinetics are controlled by

$$\alpha_m = \frac{-0.16(V+26)}{(\exp(-(V+26)/4.5)-1)}$$
$$\beta_m = \frac{0.04(V+12)}{(\exp((V+12)/10)-1)}$$
$$\tau_m = 1/(\alpha_m + \beta_m)$$
$$m_\infty = \alpha_m/(\alpha_m + \beta_m)$$
$$\alpha_h = \frac{2}{\exp((V+94)/10)}$$
$$\beta_h = \frac{8}{(\exp(-(V-68)/27)+1)}$$
$$\tau_h = 1/(\alpha_h + \beta_h)$$
$$h_\infty = \alpha_h/(\alpha_h + \beta_h).$$

A peak conductance of $\bar{g}_{Ca} = 1$ mS cm^{-2} was used when this was the only active conductance, being reduced to 0.5 mS cm^{-2} when other voltage-gated conductances were present.

The model of an A-type potassium current used is that given by Migliore *et al* (1999). Channel density increased linearly with distance from the soma to six times the proximal density after 500 μm. A peak proximal conductance of $\bar{g}_A = 0.2$ mS cm^{-2} was used here.

The model of the H-type mixed cation current is given by Borg-Graham (1998). This current is depolarizing, with a reversal potential of $E_H = -17$ mV, but is mostly activated at hyperpolarized potentials. As with the A-current, the channel density increases with distance from the soma (Magee 1999) to seven times the proximal density after 500 μm. A peak proximal conductance of $\bar{g}_H = 0.03$ mS cm^{-2} was used here.

The fast sodium and delayed-rectifier potassium current models from Bernander *et al* (1994a) were used to produce spiking in the soma to test cell output to EPSPs.

Temporal jitter: AP arrival times uniformly distributed over a small time window of 20 ms.

Quantal variance: maximum synaptic conductances varied around the mean value with a coefficient of variation of 0.3.

References

Allen C and Stevens C 1994 An evaluation of causes for unreliability of synaptic transmission *Proc. Natl Acad. Sci.* **91** 10 380–3

Amit D J 1989 *Modeling Brain Function: the World of Attractor Neural Networks* (Cambridge: Cambridge University Press)

Andreasen M and Lambert J 1999 Somatic amplification of distally generated subthreshold EPSPs in rat hippocampal pyramidal neurones *J. Physiol.* **519** 85–100

Andersen P, Silfvenius H, Sundberg S and Sveen O 1980 A comparison of distal and proximal dendritic synapses on CA1 pyramids in guinea-pig hippocampal slices in vitro *J. Physiol.* **307** 273–99

Bennett M, Gibson W and Robinson J 1994 Dynamics of the CA3 pyramidal neuron autoassociative memory network in the hippocampus *Phil. Trans. R. Soc.* B **343** 167–87

Bernander O, Douglas R, Martin K and Koch C 1991 Synaptic background activity influences spatiotemporal integration in single pyramidal cells *Proc. Natl Acad. Sci.* **88** 11 569–73

Bernander O, Koch C and Douglas R 1994a Amplification and linearization of distal synaptic input to cortical pyramidal cells *J. Neurophys.* **72** 2743–53

Bernander O, Koch C and Usher M 1994b The effect of synchronized inputs at the single neuron level *Neural Comput.* **6** 622–41

Bolshakov V and Siegelbaum S 1995 Regulation of hippocampal transmitter release during development and long-term potentiation *Science* **269** 1730–4

Borg-Graham L 1998 Interpretations of data and mechanisms for hippocampal pyramidal cell models *Cerebral Cortex Cortical Models* vol 13, ed P Ulinski, E Jones and A Peters (New York: Plenum)

Buckingham J 1991 Delicate nets, faint recollections: a study of partially connected associative network memories *PhD Thesis* University of Edinburgh

Cash S and Yuste R 1998 Input summation by cultured pyramidal neurons is linear and position-independent *J. Neurosci.* **18** 10–5

——1999 Linear summation of excitatory inputs by CA1 pyramidal neurons *Neuron* **22** 383–94

Cook E and Johnston D 1997 Active dendrites reduce location-dependent variability of synaptic input trains *J. Neurophys.* **78** 2116–28

——1999 Voltage-dependent properties of dendrites that eliminate location-dependent variability of synaptic input *J. Neurophys.* **81** 535–43

Dayan P and Willshaw D 1991 Optimising synaptic learning rules in linear associative memories *Biol. Cybern.* **65** 253–65

De Schutter E and Bower J 1994 Simulated responses of cerebellar Purkinje cells are independent of the dendritic location of granule cell synaptic inputs *Proc. Natl Acad. Sci.* **91** 4736–40

Forti L, Bossi M, Bergamaschi A, Villa A and Malgaroli A 1997 Loose-patch recordings of single quanta at individual hippocampal synapses *Nature* **388** 874–8

Gillessen T and Alzheimer C 1997 Amplification of EPSPs by low Ni^{2+}- and amiloride-sensitive Ca^{2+} channels in apical dendrites of rat CA1 pyramidal neurons *J. Neurophys.* **77** 1639–43

Graham B 1999 The effects of intrinsic noise on pattern recognition in a model pyramidal cell *ICANN99: Artificial Neural Networks (Conference Publication 470 vol 2)* pp 1006–011 (IEE)

Graham B and Willshaw D 1995 Improving recall from an associative memory *Biol. Cybern.* **72** 337–46

——1997a Capacity and information efficiency of the associative net *Network: Comput. Neural Syst.* **8** 35–54

——1997b A model of clipped Hebbian learning in a neocortical pyramidal cell *Artificial Neural Networks—ICANN '97 (Lecture Notes in Computer Science vol 1327)* ed W Gerstner, A Germond, M Hasler and J-D Nicoud (Berlin: Springer) pp 151–6

Hines M and Carnevale N 1997 The NEURON simulation environment *Neural Comput.* **9** 1179–209

Hoffman D, Magee J, Colbert C and Johnston D 1997 K^+ channel regulation of signal propagation in dendrites of hippocampal pyramidal neurons *Nature* **387** 869–75

Jensen O, Idiart M and Lisman J 1996 Physiologically realistic formation of autoassociative memory in networks with theta/gamma oscillations: role of fast NMDA channels *Learning Memory* **3** 243–56

Lipowsky R, Gillessen T and Alzheimer C 1996 Dendritic Na^+ channels amplify EPSPs in hippocampal CA1 pyramidal cells *J. Neurophys.* **76** 2181–91

Lisman J 1997 Bursts as a unit of neural information: making unreliable synapses reliable *Trends Neurosci.* **20** 38–43

Lisman J and Idiart M 1995 Storage of 7 ± 2 short-term memories in oscillatory subcycles *Science* **267** 1512–4

Magee J 1999 Dendritic I_h normalizes temporal summation in hippocampal CA1 neurons *Nature Neurosci.* **2** 508–14

Magee J and Cook E 2000 Somatic 'epsp' amplitude is independent of synapse location in hippocampal pyramidal neurons *Nature Neurosci.* **3** 895–903

Magee J, Hoffman D, Colbert C and Johnston D 1998 Electrical and calcium signaling in dendrites of hippocampal pyramidal neurons *Ann. Rev. Physiol.* **60** 327–46

Magee J and Johnston D 1995 Synaptic activation of voltage-gated channels in the dendrites of hippocampal pyramidal neurons *Science* **268** 301–4

Mainen Z, Carnevale N, Zador A, Claiborne B and Brown T 1996 Electrotonic architecture of hippocampal CA1 pyramidal neurons based on three-dimensional reconstructions *J. Neurophys.* **76** 1904–23

Major G, Evans J and Jack J 1993 Solutions for transients in arbitrarily branching cables: 1. Voltage recording with a somatic shunt *Biophys. J.* **65** 423–49

Marr D 1971 Simple memory: a theory for archicortex *Phil. Trans. R. Soc.* B **262** 23–81

McNaughton B and Morris R 1987 Hippocampal synaptic enhancement and information storage within a distributed memory system *Trends Neurosci.* **10** 408–15

Mel B 1993 Synaptic integration in an excitable dendritic tree *J. Neurophys.* **70** 1086–101

Menschik E and Finkel L 1998 Neuromodulatory control of hippocampal function: towards a model of Alzheimer's disease *Artif. Intell. Med.* **13** 99–121

Migliore M, Hoffman D, Magee J and Johnston D 1999 Role of an A-type K^+ conductance in the back-propagation of action potentials in the dendrites of hippocampal pyramidal neurons *J. Comput. Neurosci.* **7** 5–15

Stevens C and Wang Y 1995 Facilitation and depression at single central synapses *Neuron* **14** 795–802

Stricker C, Field A and Redman S 1996 Statistical analysis of amplitude fluctuations in EPSCs evoked in rat CA1 pyramidal neurones *in vitro J. Physiol.* **490** 419–41

Treves A and Rolls E 1994 Computational analysis of the role of the hippocampus in memory *Hippocampus* **4** 374–91

Turner D 1988 Waveform and amplitude characteristics of evoked responses to dendritic stimulation of CA1 guinea-pig pyramidal cells *J. Physiol.* **395** 419–39

Turner D, Chen Y, Isaac J, West M and Wheal H 1997 Excitatory synaptic site heterogeneity during paired pulse plasticity in CA1 pyramidal cells in rat hippocampus *in vitro J. Physiol.* **500.2** 441–61

Warman E, Durand D and Yuen G 1994 Reconstruction of hippocampal CA1 pyramidal cell electrophysiology by computer simulation *J. Neurophys.* **71** 2033–45

Willshaw D, Buneman O and Longuet-Higgins H 1969 Non-holographic associative memory *Nature* **222** 960–2